


Article

Decentralized Coordination Dispatch Model Based on Chaotic Mutation Harris Hawks Optimization Algorithm

Yuanyuan Wang, Zexu Yu, Zhenhai Dou ^{*}, Mengmeng Qiao, Ye Zhao, Ruishuo Xie and Lianxin Liu

School of Electrical and Electronic Engineering, Shandong University of Technology, Zibo 255000, China; 20504030537@stumail.sdut.edu.cn (Y.W.); 20504040548@stumail.sdut.edu.cn (Z.Y.); 20404010476@stumail.sdut.edu.cn (M.Q.); 20504040545@stumail.sdut.edu.cn (Y.Z.); 20504040570@stumail.sdut.edu.cn (R.X.); llxxhl6568@sdut.edu.cn (L.L.)

* Correspondence: douzhenhai@sdut.edu.cn

Abstract: Aiming at the economic dispatch problem for an interconnected system with wind power integration, and in order to realize the goals of system economy and improvement of the cross-regional consumption level of wind energy, a decentralized coordination dispatch model is established in this paper. In this model, a DC tie-line is cut by the branch cutting method and used as a coupling variable. A virtual upper-level dispatch center is established, and the economic dispatch problem to be solved is decomposed into a master optimization problem for the upper-level dispatch center and subsidiary optimization problems for the lower-level dispatch centers. For solving this model, an improved Harris hawks optimization (HHO) algorithm called the chaotic mutation Harris hawks optimization (CMHHO) algorithm is proposed. In the CMHHO algorithm, tent mapping and the “DE/pbad-to-pbest/1” strategy are introduced, and a new nonlinear escape energy factor adjustment is proposed. Through an algorithm comparison experiment and a simulation experiment with two examples, the superiority of the CMHHO algorithm, the effectiveness of the proposed model and the applicability of the CMHHO algorithm to the proposed model are verified. The model proposed is of great significance for solving the economic dispatch problem for an interconnected system with wind power integration.

Keywords: decentralized coordinated dispatch; analytical target cascading; swarm intelligence algorithm; Harris hawks optimization; optimization; DC tie-line



Citation: Wang, Y.; Yu, Z.; Dou, Z.; Qiao, M.; Zhao, Y.; Xie, R.; Liu, L. Decentralized Coordination Dispatch Model Based on Chaotic Mutation Harris Hawks Optimization Algorithm. *Energies* **2022**, *15*, 3815. <https://doi.org/10.3390/en15103815>

Academic Editor: Andrea Lazzaretto

Received: 14 April 2022

Accepted: 20 May 2022

Published: 22 May 2022

Publisher’s Note: MDPI stays neutral with regard to jurisdictional claims in published maps and institutional affiliations.



Copyright: © 2022 by the authors. Licensee MDPI, Basel, Switzerland. This article is an open access article distributed under the terms and conditions of the Creative Commons Attribution (CC BY) license (<https://creativecommons.org/licenses/by/4.0/>).

1. Introduction

In recent years, the energy crisis and environmental pollution around the world have been caused by the extensive use of fossil energy and the emission of polluting gases [1]. Due to the fact that renewable energy offers low power loss, less pollution and flexible operation, it is an important development direction for energy technology throughout the world [2]. The extensive use of renewable energy is of great significance in solving the problems of the fossil energy crisis and environmental pollution [3]. Due to the fact that wind energy has a flexible generation mode, wide distribution and low pollution, wind energy generators are widely connected to the power grid. A large number of studies have been undertaken by scholars in many countries on the optimal dispatch of integrated wind power [4].

In [5], in order to achieve wind power access and facilitate carbon trading, a low-carbon economic scheduling model function with multiple uncertainties is established, which takes into account the costs of wind power and thermal power generation, as well as the profits from carbon trading. In [6], a robust dispatch model and a robust adjustment cost model are established for the dispatch problem for large-scale wind farms. In [7], a robust optimization scheduling model considering the higher-order uncertainty of wind power is proposed to further optimize the operation cost and wind power consumption

level. In [8], in combination with practical research and data analysis, the author analyzes the influence of wind-turbine grid connection on power system scheduling. In [9], a two-stage scheduling optimization model is established to mitigate the adverse effects of grid-connected wind power on the power system stability. In [10], a low-carbon electricity scheduling model with a wind-powered grid background is established, to achieve a balance between economy and the environment, between uncertainty and certainty and between objectivity and subjectivity. All the above studies consider centralized dispatch. In 2020, the new installed wind power capacity in the global market was 93 GW, and the cumulative installed wind power capacity reached 742 GW. The total installed wind power capacity in China reached 278 GW, which is about 37% of the total installed wind power capacity in the world. However, wind resources exist mainly in the “Three North” region in China, far away from the load center. Centralized optimization is not suitable for the current situation of large-scale, high-concentration and long-distance wind power in China [11]. Decentralized coordinated dispatch is proposed to solve the dispatch problem for interconnected power systems [12–14]. The requirement for information privacy in each regional power grid is realized by the decentralized optimization algorithm [15]. In the decentralized optimization algorithm, the decoupling of the original problem is realized by exchanging a small amount of boundary information. The results obtained by decentralized solving of each sub-problem are consistent with the original problem, which ensures information privacy in each of the sub-problems and considerably reduces the computational complexity [16,17].

In [18], Lagrange relaxation (LR) is used to solve the nonlinear centralized optimization problem, which is high-dimensional, has multiple objectives and constraints and is difficult to solve; however, a large number of Lagrangian multipliers are prone to oscillation, which leads to poor convergence. In [19], augmented Lagrangian relaxation (ALR) is used to optimize a control strategy for the inverter; however, the penalty parameter and step size parameter of ALR are difficult to determine. Compared with LR and ALR, analytical target cascading (ATC) has a faster convergence rate. Considering the current situation of the large scale, high concentration and long distances of wind power in China, in this paper, the principle of ATC is used to solve the economic problems of interconnected systems with wind power.

For interconnected systems, regional decoupling and finding coupling variables are important. In [20], in order to solve the economic dispatch problem for a multi-area interconnected power system according to the principle of area decoupling, the voltage phase angle of the DC power flow model is selected as the coupling variable. However, it is difficult to deal with the DC tie-line power flow. The branch cutting method does not need to transmit the phase angle information of the boundary node, which reduces the communication transmission burden. Therefore, in this paper, the branch cutting method is used to cut the DC tie-line, and the DC tie-line power is taken as the coordination variable between regions.

In traditional dispatch, the DC tie-line operates in constant power mode, with less transmission during a load valley period and more transmission during a load peak period. In order to improve the cross-regional consumption level of wind energy in the system, in this paper, the flexible operation characteristics of the DC tie-line are considered, and the DC tie-line power is uniformly optimized.

Compared with traditional optimization methods, swarm intelligence algorithms have flexibility and robustness; they are widely used in solving complex optimization problems [21]. The ideas of swarm intelligence algorithms mostly originate from the behavior of animals, the abstract models of swarm intelligence algorithms are established by mathematical methods, the results of the algorithms are obtained by computer programming and group behaviors are formulated, improved and coordinated based on the ideas of management [22]. The new swarm intelligence algorithms have fewer parameters, faster operation speed, a simpler evolution process and stronger global search ability; they are widely used in solving multi-objective optimization problems and high-dimensional problems [23].

Examples include the artificial bee colony (ABC) algorithm, grey wolf optimization (GWO) algorithm, beetle antennae search (BAS) algorithm, cuckoo search (CS) algorithm, whale optimization algorithm (WOA) and sparrow search algorithm (SSA) [24–29].

The Harris hawks optimization (HHO) algorithm is widely used because it has a simple principle, fewer parameters and a strong global search ability [30]. In [31], the HHO algorithm is used to search PCNN parameters, and the experiment proves that the HHO algorithm can search PCNN parameters quickly and accurately. In addition, the HHO algorithm is applied to optimization dispatch, neural networks and other fields [32,33]. The characteristics of the HHO algorithm show that it can be used to solve the economic dispatch problem for an interconnected system with wind power integration.

However, like other swarm intelligence algorithms, the HHO algorithm has the drawbacks of easily falling into a local optimum and low convergence accuracy. A large number of studies have been undertaken by scholars in many countries on improving the HHO algorithm. In order to enhance the population diversity, in [34], the concept of long-term memory is integrated. In order to enhance the convergence speed, in [35], the HHO algorithm is combined with a simulated annealing algorithm. In [36], the fitness function of the HHO algorithm is improved by maximum likelihood estimation. In order to enhance the convergence accuracy, in [37], an improved strategy based on information exchange and sharing is introduced into the HHO algorithm. In order to balance local exploitation and global exploration, in [38], an elite reverse learning strategy is incorporated into the HHO algorithm.

At present, the HHO algorithm is generally improved only for one update strategy. However, the comprehensive ability to achieve improved convergence speed and accuracy, balancing local development and global search and jumping out of local optima, still needs to be improved. In this paper, in order to improve the convergence speed and accuracy of the HHO algorithm and solve the problem that the algorithm can easily fall into a local optimum, an improved HHO algorithm called the chaotic mutation Harris hawks optimization (CMHHO) algorithm is proposed. In this paper, the CMHHO algorithm is used to solve the economic dispatch problem for an interconnected system with wind power integration. In summary, aiming at the economic dispatch problem for an interconnected system with wind power integration, in order to realize the goals of system economy and improvement of the cross-regional consumption level of wind energy, a decentralized coordination dispatch model is established in this paper. In this model, according to the principle of regional decoupling, the DC tie-line is cut by the branch cutting method and used as a coupling variable. According to the principle of ATC, a virtual upper-level dispatch center is established, and the economic dispatch problem to be solved is decomposed into a master optimization problem for the upper-level dispatch center and subsidiary optimization problems for the lower-level dispatch centers. The upper-level dispatch center is responsible for coordinating the DC tie-line power flow to the interconnected regions, and the lower-level dispatch centers solve their own economic dispatch problems in a parallel manner. For this model, the CMHHO algorithm is proposed. In the CMHHO algorithm, tent mapping and the “DE/pbad-to-pbest/1” strategy are introduced, and a new nonlinear escape energy factor adjustment is proposed, which improves the convergence accuracy and convergence speed of the HHO algorithm and increases the probability of the algorithm jumping out of local optima.

The contributions of this paper are as follows:

1. The motivation for this study is to solve the economic dispatch problem for interconnected systems. In order to realize the goals of interconnected system economy and improvement of the cross-regional consumption level of wind energy in the system, a decentralized coordinated dispatch model based on the CMHHO algorithm is established.
2. In this model, according to the principle of regional decoupling, the DC tie-line is cut by the branch cutting method and used as a coupling variable.

3. In this model, according to the principle of ATC, a virtual upper-level dispatch center is established, and the economic dispatch problem to be solved is decomposed into a master optimization problem for the upper-level dispatch center and subsidiary optimization problems for the lower-level dispatch centers. The upper-level dispatch center is responsible for coordinating the DC tie-line power flow to the interconnected regions, and the lower-level dispatch centers solve their own economic dispatch problems in a parallel manner.
4. The optimization objectives, the constraint conditions and the definitions of the variables of the model are all given.
5. For solving this problem, the HHO algorithm is introduced. In order to improve the convergence speed and accuracy of the HHO algorithm and to solve the problem that the algorithm can easily fall into local optima, the CMHHO algorithm is proposed. The CMHHO algorithm is improved in three respects:
 - A new nonlinear escape energy factor renewal strategy is proposed to balance the exploitation and exploration of the algorithm;
 - A chaotic tent map is used to adjust the key parameters of the algorithm to enhance the diversity of the population;
 - A “DC/Pbad-to-Pbest/1” strategy is used to impose a global mutation operation on the population, to avoid the algorithm falling into a local optimum.
6. Through an algorithm comparison experiment and simulation of two examples, the superiority of the CMHHO algorithm, the effectiveness of the proposed model and the applicability of the CMHHO algorithm to the proposed model are verified.

The rest of the paper is organized as follows. The regional decoupling and decentralized coordination dispatch framework are described in Section 2. The definition of variables, optimization objectives and considered constraints of the decentralized coordinated dispatch model are given in Section 3. The HHO algorithm and the CMHHO algorithm are described in Section 4. The solution method for the model is described in Section 5. An algorithm comparison experiment and the case analyses are presented and discussed in Section 6. The final conclusions and recommendations for future work are listed in Section 7.

2. Regional Decoupling and Decentralized Coordination Dispatch Framework

2.1. Regional Decoupling

The key to decentralized optimization is to achieve regional scheduling independence by transmitting only the coupling information of boundary nodes to the interconnected regions. The traditional boundary node phase angle difference analysis method is generally used to decouple interconnected power systems [39]. However, it is difficult to deal with the DC tie-line power flow. Using the branch cutting method, it is not necessary to transmit the phase angle information of the boundary node, which reduces the communication transmission burden. In this paper, the branch cutting method is used to cut the DC tie-line, and the power in the DC tie-line is taken as the coordination variable between regions.

Taking a two-region interconnected system connected by a DC tie-line as an example, the boundary nodes of the two regions are defined as M and N . The branch cutting method is used to cut the DC tie-line. Equivalent DC generators m and n are connected at the boundary nodes of regions A and B , respectively, representing the operation characteristics of the DC tie-line. The principle of region decomposition is shown in Figure 1.

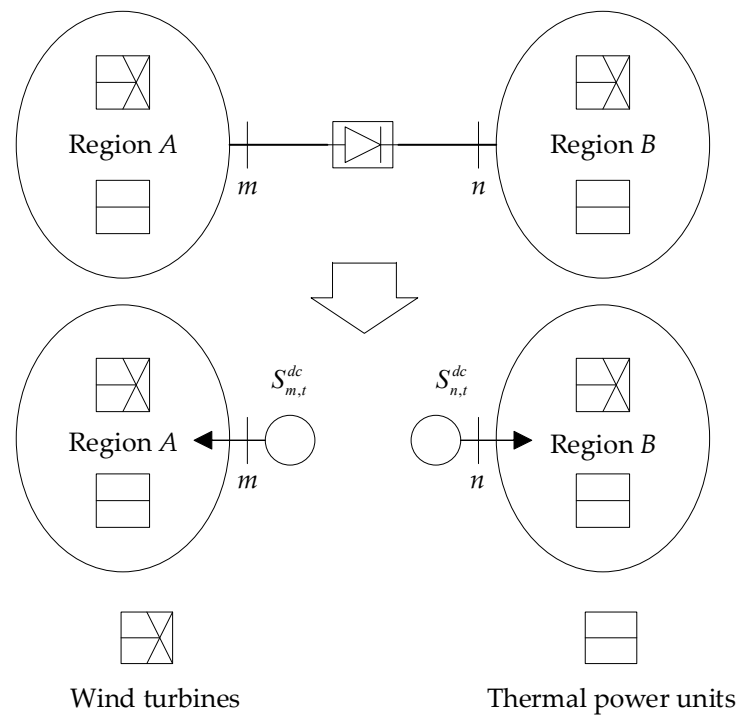


Figure 1. The principle of region decomposition.

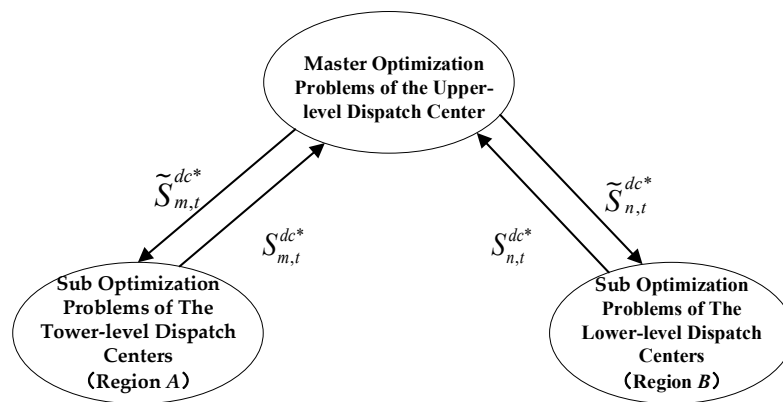
The DC tie-line is taken as the sharing and coordination variable between interconnected regions, and the following regional coupling constraints should be met in the decentralized optimization process:

$$S_{m,t}^{dc} - S_{n,t}^{dc} = 0 \tag{1}$$

where $S_{m,t}^{dc}$ and $S_{n,t}^{dc}$ are the active power output values of the equivalent DC generators m and n , respectively.

2.2. Decentralized Coordination Dispatch Framework

According to the principle of ATC, a decentralized coordination dispatch framework based on ATC was established. The decentralized coordination dispatch framework is shown in Figure 2.



*It represents the power reference value of the DC tie-line to be optimized issued by the upper and lower dispatch centers

Figure 2. Decentralized coordination dispatch framework.

A virtual upper-level dispatch center was established to realize the coordination and optimization between regions, and the economic dispatch problem to be solved was decomposed into a master optimization problem for the upper-level dispatch center and subsidiary optimization problems for the lower-level dispatch centers.

In order to ensure that the equivalent DC generators at the boundary node gradually approach equal output, a power deviation penalty term for the DC tie-line was added to the master optimization problem and the subsidiary optimization problems. In the process of decentralized coordinated dispatch, the upper-level dispatch center takes the minimum sum of the DC tie-line power deviation as the objective, obtains the optimal values of DC tie-line power and downloads these optimal values to each of the lower-level dispatch centers. Then, each lower-level dispatch center is responsible for the economic dispatch problem in its region, according to these optimal values provided by the upper-level dispatch center. Finally, each lower-level dispatch center takes the minimum cost as the objective, obtains the optimal values of the DC tie-line power and uploads these optimal values to the upper-level dispatch center for further coordination and optimization. In the whole process of decentralized coordination dispatch, the upper-level dispatch center and the lower-level dispatch centers only exchange the DC tie-line power and the multiplier information of the decentralized coordination algorithm.

3. Decentralized Coordinated Dispatch Model

This section describes the definition of variables, optimization objectives and considered constraints of the decentralized coordinated dispatch model.

3.1. Subsidiary Optimization Problems of the Lower-Level Dispatch Centers

3.1.1. The Cost of Thermal Power Units in the Interconnected System

The cost of a thermal power unit includes the operating costs, the start-up cost and the environmental pollution penalty cost of the thermal power unit. Taking thermal power unit I in region A as an example, the thermal power unit cost is

$$F_1 = v_{I,t}^A \left[\alpha_I^A (P_{I,t}^A)^2 + \beta_I^A P_{I,t}^A + \lambda_I^A \right] + v_{I,t}^A (1 - v_{I,t-1}^A) C_{I,1}^A + C_{I,2}^A P_{I,t}^A \quad (2)$$

where $v_{I,t}^A$ and $v_{I,t-1}^A$ are the start-stop states at time t and $t - 1$, respectively, set to 1 for start-up and 0 for shut-down. In addition, α_I^A , β_I^A and γ_I^A are the coefficients of the quadratic term, primary term and constant terms of the operating cost, respectively. $P_{I,t}^A$ is the output value at time t . $C_{I,1}^A$ is the coefficient of the start-up cost. $C_{I,2}^A$ is the coefficient of the environmental pollution cost [40].

3.1.2. Wind Curtailment Cost of Interconnected System

Taking wind turbine J in region A as an example, the wind curtailment cost is

$$F_2 = C_{J,3}^A P_{J,t}^{WS} \quad (3)$$

where $C_{J,3}^A$ is the coefficient of the wind curtailment cost and $P_{J,t}^{WS}$ is the abandoned air volume at time t [41].

3.1.3. DC Tie-Line Power Deviation Penalty Cost of Interconnected System

Taking the DC tie-line dc in region A as an example, the DC tie-line power deviation penalty cost is

$$F_3 = \alpha_{m,t} (\tilde{S}_{m,t}^{dc*} - S_{m,t}^{dc}) + \beta_{m,t} (\tilde{S}_{m,t}^{dc*} - S_{m,t}^{dc})^2 \quad (4)$$

where $\tilde{S}_{m,t}^{dc*}$ is the power reference value of the DC tie-line downloaded by region A , and $\alpha_{m,t}$ and $\beta_{m,t}$ are the multiplier coefficients of the algorithm.

3.1.4. Optimization Objective of Subsidiary Optimization Problems

The optimization objective of the subsidiary optimization problems is to minimize the total cost, including the costs described in (2)–(4). Taking region *A* as an example, the mathematical model is

$$\min \sum_{t=1}^T \left\{ \sum_{I=1}^{N_G^A} F_1 + \sum_{J=1}^{N_W^A} F_2 + \sum_{m=1}^{N_{dc}^A} F_3 \right\} \tag{5}$$

where *T* is the dispatching cycle and N_G^A is a collection of thermal power units in region *A*. N_W^A is a collection of wind turbines in region *A*. N_{dc}^A is a collection of DC tie-line nodes in region *A*.

3.1.5. Constraints of Subsidiary Optimization Problems

1. Power balance constraints.

$$\sum_{I=1}^{N_G^A} P_{I,t}^A + \sum_{J=1}^{N_W^A} (P_{J,t}^W - P_{J,t}^{WS}) - K \sum_{m=1}^{N_{dc}^A} S_{m,t}^{dc} = \sum_{k=1}^{N_D^A} P_{k,t}^D \tag{6}$$

where $P_{J,t}^W$ is the predicted output value of wind turbine *J* at time *t*. *K* represents the rectifier and inverter signs of the converter. N_D^A is a collection of load nodes in region *A*. $P_{k,t}^D$ is the predictive value of load *k* at time *t*.

2. Output constraint of thermal power units.

$$P_{I,t}^{Amin} \leq P_{I,t}^A \leq P_{I,t}^{Amax} \tag{7}$$

where $P_{I,t}^{Amin}$ and $P_{I,t}^{Amax}$ are the minimum and maximum allowable output values of thermal power unit *I* at time *t*, respectively.

3. Climbing and landslide constraints of thermal power units.

$$R_{DI}^A T \leq P_{I,t}^A - P_{I,t-1}^A \leq R_{UI}^A T \tag{8}$$

where R_{DI}^A and R_{UI}^A are the landslide rate and climbing rate of thermal power unit *I*, respectively. $P_{I,t-1}^A$ is the output value of thermal power unit *I* at time *t* – 1 [42].

4. Output constraints of wind turbines.

$$P_{J,t}^{Wmin} \leq P_{J,t}^W \leq P_{J,t}^{Wmax} \tag{9}$$

where $P_{J,t}^{Wmin}$ and $P_{J,t}^{Wmax}$ are the minimum and maximum allowable output values of wind turbine *J* at time *t*, respectively.

5. Positive and negative spinning reserve constraints.

$$\begin{cases} \sum_{I=1}^{N_G^A} \min [P_{I,t}^{Amax}, (P_{I,t}^A + R_{UI}^A) v_{I,t}^A] + \sum_{J=1}^{N_W^A} (P_{J,t}^W - P_{J,t}^{WS}) \geq \sum_{k=1}^{N_D^A} P_{k,t}^D + K \sum_{m=1}^{N_{dc}^A} \sum_{n=1}^{N_{dc}^B} S_{mn}^{dc} + R_t^{A+} \\ R_t^{A+} = \omega_D \sum_{k=1}^{N_D^A} P_{k,t}^D + \omega_u \sum_{J=1}^{N_W^A} P_{J,t}^W \end{cases} \tag{10}$$

$$\begin{cases} \sum_{I=1}^{N_G^A} \min [P_{I,t}^{Amin}, (P_{I,t}^A - R_{DI}^A) v_{I,t}^A] + \sum_{J=1}^{N_W^A} (P_{J,t}^W - P_{J,t}^{WS}) \geq R_t^{A-} - \sum_{k=1}^{N_D^A} P_{k,t}^D - K \sum_{m=1}^{N_{dc}^A} \sum_{n=1}^{N_{dc}^B} S_{mn}^{dc} \\ R_t^{A-} = \omega_d \sum_{J=1}^{N_W^A} (P_{J,t}^{Wmax} - P_{J,t}^W) \end{cases} \tag{11}$$

where N_{dc}^B is a collection of DC tie-line nodes in region B . \bar{S}_{mn}^{dc} and \underline{S}_{mn}^{dc} are the upper and lower limits of the DC tie-line output at time t , respectively. R_t^{A+} and R_t^{A-} are the positive and negative spinning reserve capacities required by region A at time t , respectively, ω_u and ω_d are the positive and negative reserve factors of wind power and ω_D is the load reserve factor [43].

6. Minimum start–stop time constraint of thermal power units.

$$\begin{cases} \left(V_{I,t-1}^A V_{I,t}^A \right) \left(T_{I,t-1}^{on} T_I^{on} \right) \geq 0 \\ \left(V_{I,t}^A V_{I,t-1}^A \right) \left(T_{I,t-1}^{off} T_I^{off} \right) \geq 0 \end{cases} \quad (12)$$

where $T_{I,t-1}^{on}$ and $T_{I,t-1}^{off}$ are the continuous operation and outage times of thermal power unit I in the $t - 1$ period, respectively. T_I^{on} and T_I^{off} are the minimum operation and outage times of thermal power unit I , respectively [44].

7. Power flow safety constraints.

$$\left| \sum_{I=1}^{N_G^A} F_{li}^G P_{I,t}^A + \sum_{j=1}^{N_W^A} F_{lj}^W \left(P_{j,t}^W - P_{j,t}^{WS} \right) - K \sum_{m=1}^{N_{dc}^A} F_{lm}^{dc} S_{m,t}^{dc} - \sum_{k=1}^{N_D^A} F_{lk}^D P_{k,t}^D \right| \leq \bar{F}_L \quad (13)$$

where F_{li}^G , F_{lj}^G , F_{lm}^G and F_{lk}^G are the power flow transfer distribution factors of thermal power unit I , wind power unit J , equivalent generator m and load k , respectively. \bar{F}_L is the maximum transmitted power on line L .

8. DC tie-line constraints.

In order to fully tap the interaction potential between interconnected power systems and improve the cross-regional consumption level of wind power, the output of the DC tie-line is optimized in this paper. Taking the equivalent generator m as an example, the constraints that must be met can be found in [45,46] and will not be repeated here.

3.2. Master Optimization Problem of the Upper-Level Dispatch Center

The upper-level dispatch center takes the minimum sum of the DC tie-line power deviations as the optimization objective, updates the reference values of the DC tie-line and sends them to each lower-level dispatch center for the next optimization. The objective of the master optimization problem is

$$\min \left\{ \sum_{m=1}^{N_{dc}^A} \left[\alpha_{m,t} \left(\tilde{S}_{m,t}^{dc} - S_{m,t}^{dc*} \right) + \beta_{m,t} \left(\tilde{S}_{m,t}^{dc} - S_{m,t}^{dc*} \right)^2 \right] + \sum_{n=1}^{N_{dc}^B} \left[\alpha_{n,t} \left(\tilde{S}_{n,t}^{dc} - S_{n,t}^{dc*} \right) + \beta_{n,t} \left(\tilde{S}_{n,t}^{dc} - S_{n,t}^{dc*} \right)^2 \right] \right\} \quad (14)$$

where $\tilde{S}_{m,t}^{dc}$ and $\tilde{S}_{n,t}^{dc}$ are the outputs of the equivalent DC generators m and n at time t , respectively. These are the power reference values for the DC tie-line to be optimized. $S_{m,t}^{dc*}$ and $S_{n,t}^{dc*}$ are the power reference values of the DC tie-line uploaded by the lower-level dispatch centers.

The regional coupling condition is

$$\tilde{S}_{m,t}^{dc} + \tilde{S}_{n,t}^{dc} = 0 \quad (15)$$

4. Improvements to HHO Algorithm

This section describes the steps of the traditional HHO algorithm and the CMHHO algorithm proposed in this paper and shows the associated flow charts.

4.1. Basic Harris Hawks Optimization Algorithm

The HHO algorithm is a metaheuristic algorithm, inspired by the cooperative foraging behavior of eagles. A specific description of each phase is given in the following sections.

4.1.1. Exploration Phase of HHO Algorithm

The exploration phase is a global search process. In this phase, eagles randomly appear at a certain position in the search space and move to the optimal solution according to the two equal-opportunity strategies, finally finding a suitable location around the prey and completing the encirclement. The mathematical formula is

$$X(t + 1) = \begin{cases} X_{rand}(t) - r_1|X_{rand}(t) - 2r_2X(t)| & q \geq 0.5 \\ X_{rabbit}(t) - X_m(t) - r_3[lb - r_4(ub - lb)] & q < 0.5 \end{cases} \tag{16}$$

$$X_m(t) = \frac{1}{N} \sum_{i=1}^N X_i(t) \tag{17}$$

where $X_{rand}(t)$ is a random individual in the population of iteration t . $X_{rabbit}(t)$ is the position of the optimal individual in the current population. $X_m(t)$ is the average value of the positions in the current population, and ub and lb are the upper and lower boundary values of the population, respectively. N is the population size and q is a random number with a uniform distribution in the range $(0, 1)$. When $q < 0.5$, the eagles will move according to the positions of the other members of the population and the prey. When $q \geq 0.5$, the eagles will randomly inhabit trees within the range of the population's activity [47].

4.1.2. Transition from Exploration to Exploitation of HHO Algorithm

The transition process from global exploration to local exploitation depends on the escape energy factor E . The expression for the escape energy factor is

$$E = 2E_0 \left(1 - \frac{t}{T} \right) \tag{18}$$

where E_0 is a random number in the range $(0, 1)$, and t and T are the current iteration and the maximum number of iterations, respectively. When $|E| \geq 1$, the HHO algorithm performs a global search. When $|E| < 1$, the HHO algorithm turns to the exploitation stage representing a local search [48].

4.1.3. Exploitation Stage of HHO Algorithm

After the eagles complete the siege of the target prey, they attack during the exploitation stage. In this stage, four different strategies are used to simulate the hunting behavior. E and r are combined to determine the specific strategies. The term r represents the chance of the prey escaping and is a random number in the range $(0, 1)$. When $r < 0.5$, the prey can escape from the encirclement. When $r \geq 0.5$, the prey cannot escape from the encirclement [49].

1. Soft besiege HHO algorithm.

When $0.5 < |E| \leq 1$ and $r \geq 0.5$, the prey has enough physical strength and tries to escape but is eventually captured. The calculation formula is

$$X(t + 1) = \Delta X(t) - E|JX_{rand}(t) - X(t)| \tag{19}$$

$$\Delta X(t) = X_{rabbit}(t) - X(t) \tag{20}$$

$$J = 2(1 - r_5) \tag{21}$$

where $\Delta X(t)$ is the vector distance between the optimal individual and the current individual and r_5 is a random number with a uniform distribution in the range $(0, 1)$. J is the optimal individual jump distance.

2. Soft besiege HHO algorithm.

When $|E| < 0.5$ and $r \geq 0.5$, the prey does not have sufficient energy and is directly captured by the eagle. The calculation formula is

$$X(t + 1) = X_{rabbitt}(t) - E|\Delta X(t)| \tag{22}$$

3. Soft besiege with progressive rapid dives HHO algorithm.

When $0.5 \leq |E| \leq 1$ and $r < 0.5$, the prey has escape energy and has a chance to escape, and the eagles form a soft encirclement. The calculation formula is

$$X(t + 1) = \begin{cases} Y = X_{rabbitt}(t) - E|JX_{rabbitt}(t) - X(t)| & F(Y) < F[X(t)] \\ Z = Y + S \times LF(D) & F(Z) < F[X(t)] \end{cases} \tag{23}$$

where D is the dimension of the problem and S is a D -dimensional random vector. LF is the Levy flight function and its formula is

$$\begin{cases} LF(x) = 0.01 \times \frac{ru \times \sigma}{|rv|^{\frac{1}{\beta}}} \\ \sigma = \left\{ \frac{r(1+\beta) \times \sin(\frac{\pi\beta}{2})}{r(\frac{1+\beta}{2}) \times \beta \times 2^{(\frac{\beta-1}{2})}} \right\}^{\frac{1}{\beta}} \end{cases} \tag{24}$$

where ru and rv are random numbers in the range $(0, 1)$ and β is a constant with a value of 1.5.

4. Hard besiege with progressive rapid dives HHO algorithm.

When $|E| < 0.5$ and $r < 0.5$, the prey has escape energy and has a chance to escape, and the eagles form a hard encirclement. The calculation formula is

$$X(t + 1) = \begin{cases} Y = X_{rabbitt}(t) - E|JX_{rabbitt}(t) - X_m(t)| & F(Y) < F[X(t)] \\ Z = Y + S \times LF(D) & F(Z) < F[X(t)] \end{cases} \tag{25}$$

The flow chart of the HHO algorithm is shown in Figure 3.

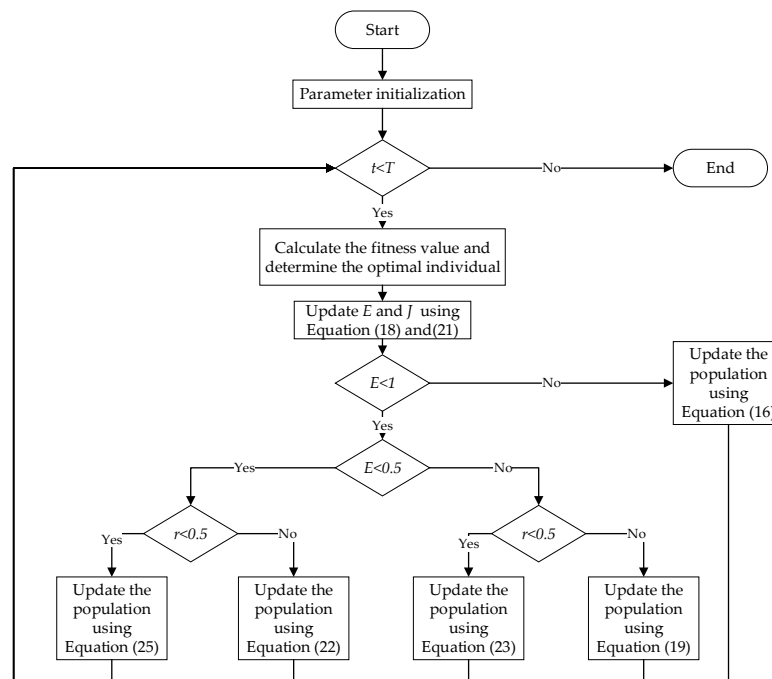


Figure 3. The flow chart of the HHO algorithm.

4.2. Chaotic Mutation Harris Hawks Optimization

At present, the HHO algorithm has generally only been improved for a certain update strategy of the algorithm. However, the comprehensive ability to improve the convergence speed and accuracy, balancing the local development and global search and jumping out of local optima, still needs to be improved. In this paper, in order to improve the convergence speed and accuracy of the HHO algorithm and solve the problem that the algorithm can easily fall into a local optimum, the HHO algorithm is improved in three respects, and the CMHHO algorithm is proposed. The specific improvements are as follows.

4.2.1. New Nonlinear Escape Energy Factor Update Strategy of CMHHO Algorithm

The transition from exploration to exploitation in the HHO algorithm is mainly controlled by the escape energy factor E . The energy factor update strategy of the HHO algorithm is in a linearly decreasing state. The HHO algorithm only performs a local search in the second half of the iteration, where it is easy to fall into a local optimum. In order to better balance the exploration and development capabilities, a new nonlinear escape energy factor update strategy is proposed. The calculation formula is

$$E = E_0 \exp\left(-\frac{t}{T}\right) \quad (26)$$

4.2.2. Tent Mapping Initialization in CMHHO Algorithm

Tent mapping is a nonlinear dynamic discrete chaotic mapping system, with uniform distribution characteristics and good correlation. The calculation formula is

$$r(t+1) = \begin{cases} \frac{r(t)}{\alpha} & r(t) \in [0, \alpha] \\ \frac{1-r(t)}{1-\alpha} & r(t) \in [\alpha, 1] \end{cases} \quad (27)$$

where α is a random number in the range $(0, 1)$ [50].

The mapping distribution for $\alpha = 0.4$ is shown in Figure 4. It can be seen from Figure 4 that the distribution has high uniformity and randomness.

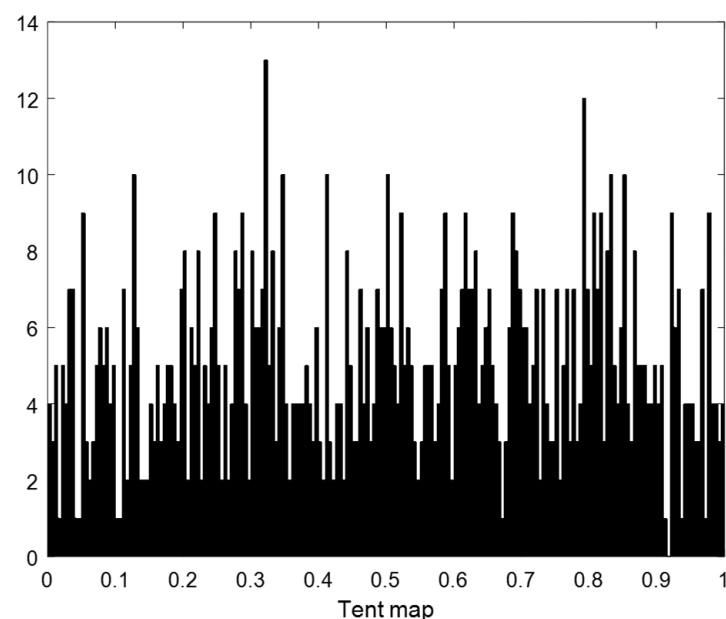


Figure 4. The mapping distribution for $\alpha = 0.4$.

The parameter r in the HHO algorithm represents the chance of escape of the prey and is a random number in the range $(0, 1)$. In this paper, a chaotic tent map is used to adjust the value of the key parameter r of the CMHHO algorithm. The update formula is

$$r_{i+1} = \begin{cases} \frac{r_i}{0.4} & x_i < 0.4 \\ \frac{1-r_i}{0.6} & x_i \geq 0.4 \end{cases} \quad (28)$$

4.2.3. Mutation Strategy “DE/pbad-to-pbest/1” of the CMHHO Algorithm

The “DE/pbad-to-pbest/1” mutation strategy utilizes not only the good solution information (pbest) but also the information on the bad solution (pbad) with respect to the good solution, to balance exploration and exploitation. This mutation strategy utilizes the good solution information to speed up the convergence rate in the exploration phase. It then utilizes the information on the bad solution with respect to the good solution to increase the diversity of the population and the probability of jumping out of a local optimum.

The HHO algorithm directly enters the next iteration after the exploitation stage, resulting in a poor population search ability at the end stage. In order to increase the diversity of the population and enhance the search ability of the terminal population, the “DE/pbad-to-pbest/1” mutation strategy was introduced, to impose a global mutation operation on the population at the end of each iteration. The calculation formula is

$$V_{i,G} = X_{i,G} + F(X_{pbest,G} - X_{pbad,G}) \quad (29)$$

where $V_{i,G}$ is the new population created by the mutation. $X_{i,G}$ is a random individual in the current population. F is a mutation factor, which is a random number with a uniform distribution in the range $(0, 1)$. $X_{pbest,G}$ is a random individual from among the best $100p\%$ individuals, $X_{pbad,G}$ is a random individual from among the worst $100p'\%$ individuals, and p and p' are random numbers in the range $(0, 1)$ [51].

The specific flow chart for the CMHHO algorithm is shown in Figure 5.

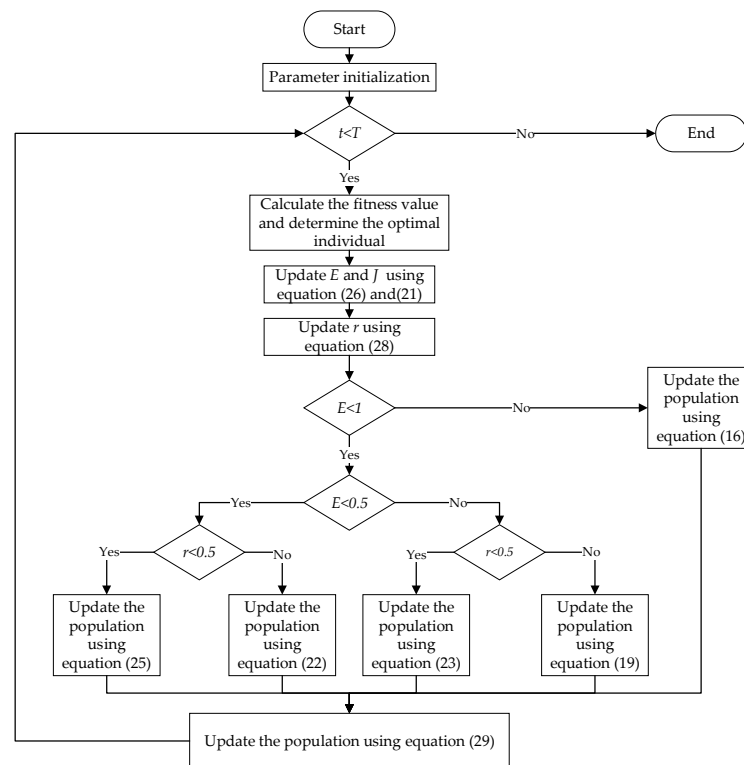


Figure 5. The flow chart of the CMHHO algorithm.

5. Solution Method of Model

This section describes the solution method of the model, including the algorithm convergence criterion, the multiplier coefficients update formula, the steps for solving the model and the flow chart of the model.

5.1. Algorithm Convergence Criterion

The convergence criterion of the algorithm used in this paper is

$$\begin{cases} \frac{|\tilde{S}_{m,t}^{dc*}(\tau) - S_{m,t}^{dc*}(\tau)|}{\bar{S}_{mn}^{dc}} \leq \varepsilon \\ \frac{|\tilde{S}_{n,t}^{dc*}(\tau) - S_{n,t}^{dc*}(\tau)|}{\bar{S}_{mn}^{dc}} \leq \varepsilon \end{cases} \quad (30)$$

where ε is the convergence accuracy.

5.2. Multiplier Coefficients Update Formula

If the convergence condition is not satisfied after τ iterations, the multiplier coefficients are updated according to Formula (31) and then sent to each lower-level center for the next iteration. The multiplier coefficients update formula is

$$\begin{cases} \alpha_{m,t}(\tau) = \alpha_{m,t}(\tau - 1) + 2\beta_{m,t}(\tau - 1)^2 [\tilde{S}_{m,t}^{dc*}(\tau - 1) - S_{m,t}^{dc*}(\tau - 1)] \\ \beta_{m,t}(\tau) = \gamma\beta_{m,t}(\tau - 1) \\ \alpha_{n,t}(\tau) = \alpha_{n,t}(\tau - 1) + 2\beta_{n,t}(\tau - 1)^2 [\tilde{S}_{n,t}^{dc*}(\tau - 1) - S_{n,t}^{dc*}(\tau - 1)] \\ \beta_{n,t}(\tau) = \gamma\beta_{n,t}(\tau - 1) \end{cases} \quad (31)$$

where γ is a constant with a value generally between 1 and 3. The initial values of $\alpha_{m,t}$ and $\beta_{m,t}$ generally take smaller constants, satisfying $1 \leq \alpha_{m,t} \leq \beta_{m,t}$ [52].

5.3. Solution Steps and Flowchart of Model

The solution steps of the model are as follows, and the flow chart of the model is shown in Figure 6.

Step 1: Set $\tau = 1$. The DC tie-line power values $\tilde{S}_{m,t}^{dc*}(\tau - 1)$ and $\tilde{S}_{n,t}^{dc*}(\tau - 1)$ and the multiplier coefficients $\alpha_{m,t}(\tau - 1)$ and $\beta_{m,t}(\tau - 1)$ are initialized and sent to the corresponding lower-level dispatch centers by the upper-level dispatch center.

Step 2: Each lower-level dispatch center uses the CMHHO algorithm to independently solve the economic dispatch problem in their own region, with the goal of minimizing the total cost. The optimum values of the DC tie-line power $S_{m,t}^{dc*}(\tau)$ and $S_{n,t}^{dc*}(\tau)$ are obtained by each lower-level dispatch center and uploaded to the upper-level dispatch center.

Step 3: The upper-level dispatch center uses the CMHHO algorithm to solve the master optimization problem according to the DC tie-line power values $S_{m,t}^{dc*}(\tau)$ and $S_{n,t}^{dc*}(\tau)$ uploaded by each lower-level center, aiming at the minimum sum of tie-line power deviations. The reference values of the DC tie-line power $\tilde{S}_{m,t}^{dc*}(\tau)$ and $\tilde{S}_{n,t}^{dc*}(\tau)$ are updated and downloaded to the corresponding lower-level dispatch center again.

Step 4: Whether the convergence condition is satisfied is determined using Equation (30). If the convergence condition is satisfied, the iteration ends and the result is the optimal solution. If the convergence condition is not satisfied, proceed to step 5 for the next iteration.

Step 5: Set $\tau = \tau + 1$, update the algorithm multipliers $\alpha_{m,t}(\tau)$ and $\beta_{m,t}(\tau)$ using Equation (31) and then return to step 2 for the next iteration.

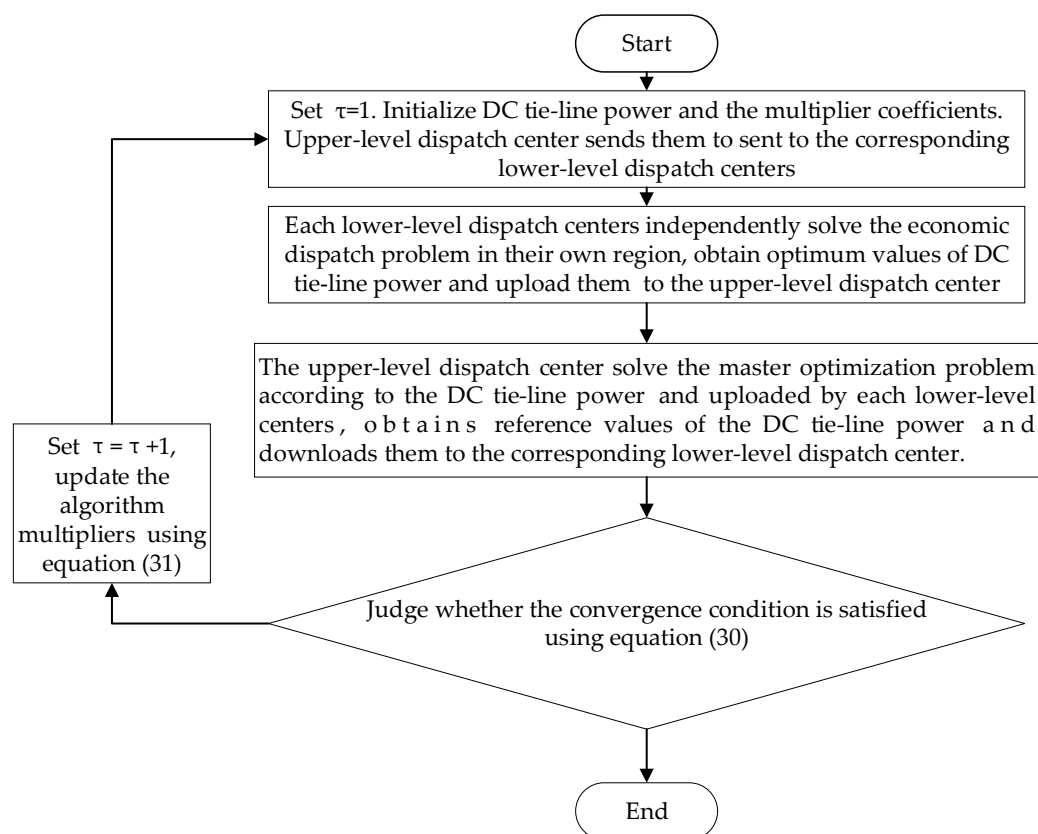


Figure 6. The flow chart of the model.

6. Experiment and Analysis

The decentralized coordinated dispatch model of a multi-region power system with wind power integration is a mixed-integer programming problem. The YALMIP platform was used to set up the model in MATLAB. The master optimization problem and the subsidiary optimization problems are solved by the CMHHO algorithm. First, in order to verify the superiority of the CMHHO algorithm, an algorithm comparison experiment and analysis was undertaken. Then, in order to verify the effectiveness of the proposed model and the applicability of the CMHHO algorithm to the proposed model, a two-region 6-node interconnected system and a two-region 78-node interconnected system were established. This section describes the simulation experiment and the analysis of the results.

6.1. Algorithm Comparison Experiment

In order to verify the effectiveness and superiority of the CMHHO algorithm, the WOA, SSA, GWO, HHO and CMHHO algorithms were selected to conduct an algorithm comparison experiment on 12 test functions. This set of benchmark functions included five unimodal functions, three multimodal functions and four multimodal functions with fixed dimensions. The specific information for the test functions is shown in Table 1.

Table 1. Test functions specific information.

Test Function	Type	Dimension	Scope	Optimal Value
$f_1 = \sum_{i=1}^D x_i^2$	US	—	[−100, 100]	0
$f_2 = \sum_{i=1}^D x_i + \prod_{i=1}^D x_i $	UN	—	[−10, 10]	0
$f_3 = \sum_{i=1}^D \left(\sum_{j=1}^D x_{ij} \right)^2$	UN	—	[−100, 100]	0
$f_4 = \max_i \{ x_i , 1 \leq i \leq D\}$	US	—	[−100, 100]	0
$f_5 = \sum_{i=1}^D ix_i^4 + \text{random}(0,1)$	US	—	[−1.28, 1.28]	0
$f_6 = \sum_{i=1}^D [x_i^2 - 10 \cos(2\pi x_i) + 10]$	MS	—	[−5.12, 5.12]	0
$f_7 = 20 + e - 20 \exp\left(-0.2 \sqrt{\frac{1}{D} \sum_{i=1}^D x_i^2}\right) - \exp\left(\frac{1}{D} \sum_{i=1}^D \cos(2\pi x_i)\right)$	MS	—	[−32, 32]	8.8818×10^{-16}
$f_8 = \frac{1}{4000} \sum_{i=1}^D x_i^2 - \prod_{i=1}^D \cos\left(\frac{x_i}{\sqrt{i}}\right) + 1$	MN	—	[−600, 600]	0
$f_9 = \left(x_2 - \frac{5}{4\pi^2} x_1^2 + \frac{5}{\pi} x_1 - 6\right)^2 + 10 \left(1 - \frac{1}{8\pi}\right) \cos x_1 + 10$	MS	2	[−5, 10] × [0, 15]	0.398
$f_{10} = \left[1 + (x_1 + x_2 + 1)^2 - (19 - 14x_1 + 3x_1^2 - 14x_2 + 6x_1x_2 + 3x_2^2)\right] \times \left[30 + (2x_1 - 3x_2)^2(18 - 32x_1 + 12x_1^2 - 48x_2 - 36x_1x_2 + 27x_2^2)\right]$	MN	2	[−5, 5]	3
$f_{11} = -\sum_{i=1}^4 c_i \exp\left(-\sum_{j=1}^3 a_{ijj} (x_i - p_{ij})^2\right)$	MN	3	[0, 1]	−3.8628
$f_{12} = -\sum_{i=1}^{10} \left[(X - a_i)(X - a_i)^T + c_i\right]^{-1}$	MN	4	[0, 10]	−10.5364

The test experiments were performed on the same experimental platform, and all algorithms were programmed using MATLAB R2018b. The dimensions of the test functions f_1 – f_8 were all 30, and the dimensions of the test functions f_9 – f_{12} were consistent with those in Table 1. The number of populations was set to 30, the maximum number of iterations was 500 and other parameters for the comparison algorithms were consistent with the original literature. The WOA, GWO, SSA, HHO and CMHHO algorithms were independently run 30 times on each test function, and the test results for the different algorithms are shown in Table 2.

Table 2. Comparison of test results of different algorithms.

Test Function	Algorithm	Optimal Value	Average Value	Standard Deviation
f_1	WOA	1.49×10^{-85}	3.65×10^{-74}	1.53×10^{-73}
	SSA	1.40×10^{-290}	4.92×10^{-07}	1.46×10^{-03}
	GWO	4.36×10^{-294}	9.88×10^{-28}	1.55×10^{-27}
	HHO	2.78×10^{-1110}	3.19×10^{-98}	1.22×10^{-97}
	CMHHO	2.52×10^{-249}	6.35×10^{-214}	0
f_2	WOA	4.04×10^{-58}	2.75×10^{-51}	8.99×10^{-51}
	SSA	3.99×10^{-194}	6.95×10^{-04}	2.02×10^{-3}
	GWO	1.18×10^{-17}	9.66×10^{-17}	7.46×10^{-17}
	HHO	1.05×10^{-60}	1.90×10^{-47}	1.04×10^{-46}
	CMHHO	8.07×10^{-127}	9.42×10^{-112}	2.79×10^{-111}
f_3	WOA	1.30×10^{-4}	4.29×10^4	1.60×10^4
	SSA	8.07×10^{-195}	5.54×10^5	2.52×10^{-4}
	GWO	3.45×10^{-8}	8.57×10^{-6}	3.16×10^{-5}
	HHO	1.55×10^{-98}	1.23×10^{-77}	5.38×10^{-77}
	CMHHO	3.54×10^{-211}	1.06×10^{-155}	5.80×10^{-151}

Table 2. Cont.

Test Function	Algorithm	Optimal Value	Average Value	Standard Deviation
f ₄	WOA	1.24×10^{-3}	3.80×10^1	2.71×10^1
	SSA	1.92×10^{-178}	4.82×10^{-5}	1.34×10^{-4}
	GWO	1.22×10^{-7}	5.88×10^{-7}	5.97×10^{-7}
	HHO	3.43×10^{-57}	5.66×10^{-49}	1.92×10^{-48}
	CMHHO	4.31×10^{-123}	3.54×10^{-112}	1.84×10^{-111}
f ₅	WOA	6.12×10^{-5}	3.93×10^{-3}	4.85×10^{-3}
	SSA	6.19×10^{-4}	3.54×10^{-3}	3.13×10^{-3}
	GWO	3.15×10^{-4}	1.91×10^{-3}	1.27×10^{-3}
	HHO	3.17×10^{-6}	1.74×10^{-4}	1.48×10^{-4}
	CMHHO	9.67×10^{-6}	1.61×10^{-4}	1.99×10^{-5}
f ₆	WOA	0	8.97	3.70×10^1
	SSA	0	1.17×10^{-4}	5.85×10^{-4}
	GWO	5.68×10^{-14}	1.44	2.01
	HHO	0	0	0
	CMHHO	0	0	0
f ₇	WOA	8.88×10^{-16}	3.84×10^{-15}	1.89×10^{-15}
	SSA	8.88×10^{-16}	2.08×10^{-4}	5.85×10^{-4}
	GWO	7.55×10^{-14}	-1.10×10^8	1.12×10^8
	HHO	8.88×10^{-16}	8.88×10^{-16}	0
	CMHHO	8.88×10^{-16}	8.88×10^{-16}	0
f ₈	WOA	0	7.53×10^{-3}	2.93×10^{-2}
	SSA	0	1.58×10^{-7}	3.83×10^{-2}
	GWO	0	5.27×10^{-3}	1.13×10^{-2}
	HHO	0	0	0
	CMHHO	0	0	0
f ₉	WOA	3.98×10^{-1}	3.98×10^{-1}	2.89×10^{-5}
	SSA	3.98×10^{-1}	4.08×10^{-1}	1.79×10^{-2}
	GWO	3.98×10^{-1}	3.98×10^{-1}	4.05×10^{-6}
	HHO	3.98×10^{-1}	3.98×10^{-1}	1.79×10^{-5}
	CMHHO	3.98×10^{-1}	3.98×10^{-1}	1.77×10^{-5}
f ₁₀	WOA	3.00	3.00	1.54
	SSA	3.00	8.02	1.03×10^1
	GWO	3.00	3.00	3.95×10^{-5}
	HHO	3.00	3.00	1.55×10^{-6}
	CMHHO	3.00	3.00	1.44×10^{-6}
f ₁₁	WOA	-3.86	-3.86	8.00×10^{-3}
	SSA	-3.86	-3.76	1.73×10^{-1}
	GWO	-3.86	-3.86	2.73×10^{-3}
	HHO	-3.86	-3.86	5.64×10^{-3}
	CMHHO	-3.86	-3.86	1.76×10^{-3}
f ₁₂	WOA	-1.05×10^1	-6.02	3.05
	SSA	-1.05×10^1	-9.45	2.04
	GWO	-1.05×10^1	-1.04×10^1	9.87×10^{-1}
	HHO	-5.13	-5.12	5.31×10^{-1}
	CMHHO	-1.03×10^1	-6.22	1.98

For f₁–f₅, the average value obtained by the CMHHO algorithm is the closest to the optimal value, and the standard deviation obtained by the CMHHO algorithm is the lowest. In solving the unimodal function problem, the CMHHO algorithm has higher accuracy, less data fluctuation during the optimization process and stronger robustness. For f₆–f₈, the CMHHO algorithm, HHO algorithm, SSA algorithm and GWO algorithm can all find the optimal value, the average value obtained by CMHHO algorithm and the HHO algorithm

is the closest to the optimal value, and the standard deviation obtained by the CMHHO algorithm and HHO algorithm is 0. For f_9 – f_{11} , the CMHHO algorithm, HHO algorithm, GWO algorithm and WOA algorithm can all find the optimal value, and the standard deviation obtained by the CMHHO algorithm is the lowest. For f_{12} , the average value obtained by the SSA is the closest to the optimal value, followed by the CMHHO algorithm, and the standard deviation obtained by the CMHHO algorithm is the lowest. In solving multimodal function problems, the CMHHO algorithm has a better global search ability and better ability to avoid premature convergence.

The convergence curves of the five algorithms are shown in Figure 7. For f_1 – f_5 , the convergence accuracy and convergence speed of the CMHHO algorithm are greatly improved compared with the other algorithms. For f_5 , there are multiple inflection points in the iterative process of the CMHHO algorithm, which proves that the improved algorithm can easily jump out of a local optimum and has a better global optimization effect. For f_6 , the CMHHO algorithm, HHO algorithm and GWO algorithm converge to the optimal value, and the convergence speed of the CMHHO algorithm is greatly improved compared with the other algorithms. For f_7 , the convergence speed of the CMHHO algorithm is greatly improved compared with the other algorithms, and the convergence accuracy of the HHO algorithm is the best, followed by the CMHHO algorithm. For f_8 , except for SSA, the algorithms converge to the optimal value, and the convergence speed of the CMHHO algorithm is greatly improved compared with the other comparison algorithms. For f_9 and f_{11} , five algorithms have similar convergence accuracies, and the convergence speed of the CMHHO algorithm is slightly faster than the other algorithms. For f_{10} , except for the SSA algorithm, the algorithms have similar convergence accuracies, and the convergence rates of the five algorithms are similar. For f_{12} , except for the HHO algorithm, the algorithms converge to the optimal value, and the convergence speed of the SSA algorithm is the best, followed by the CMHHO algorithm. This shows that the robustness of the CMHHO algorithm is strong.

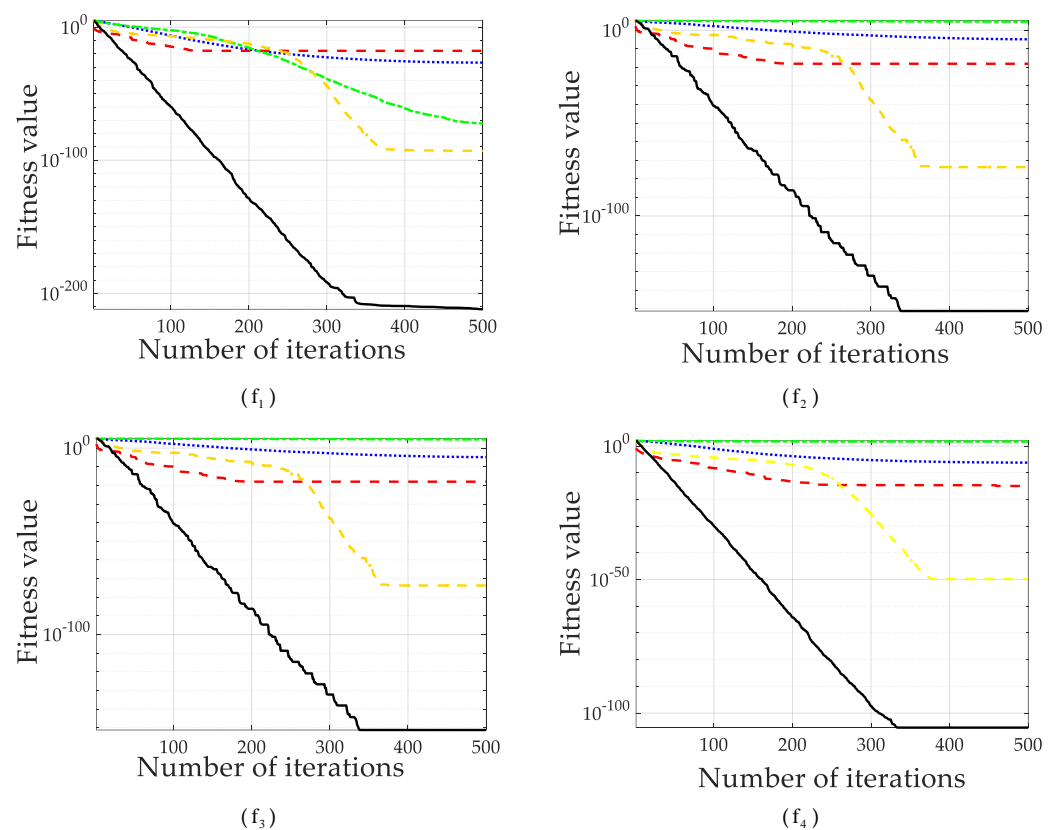


Figure 7. Cont.

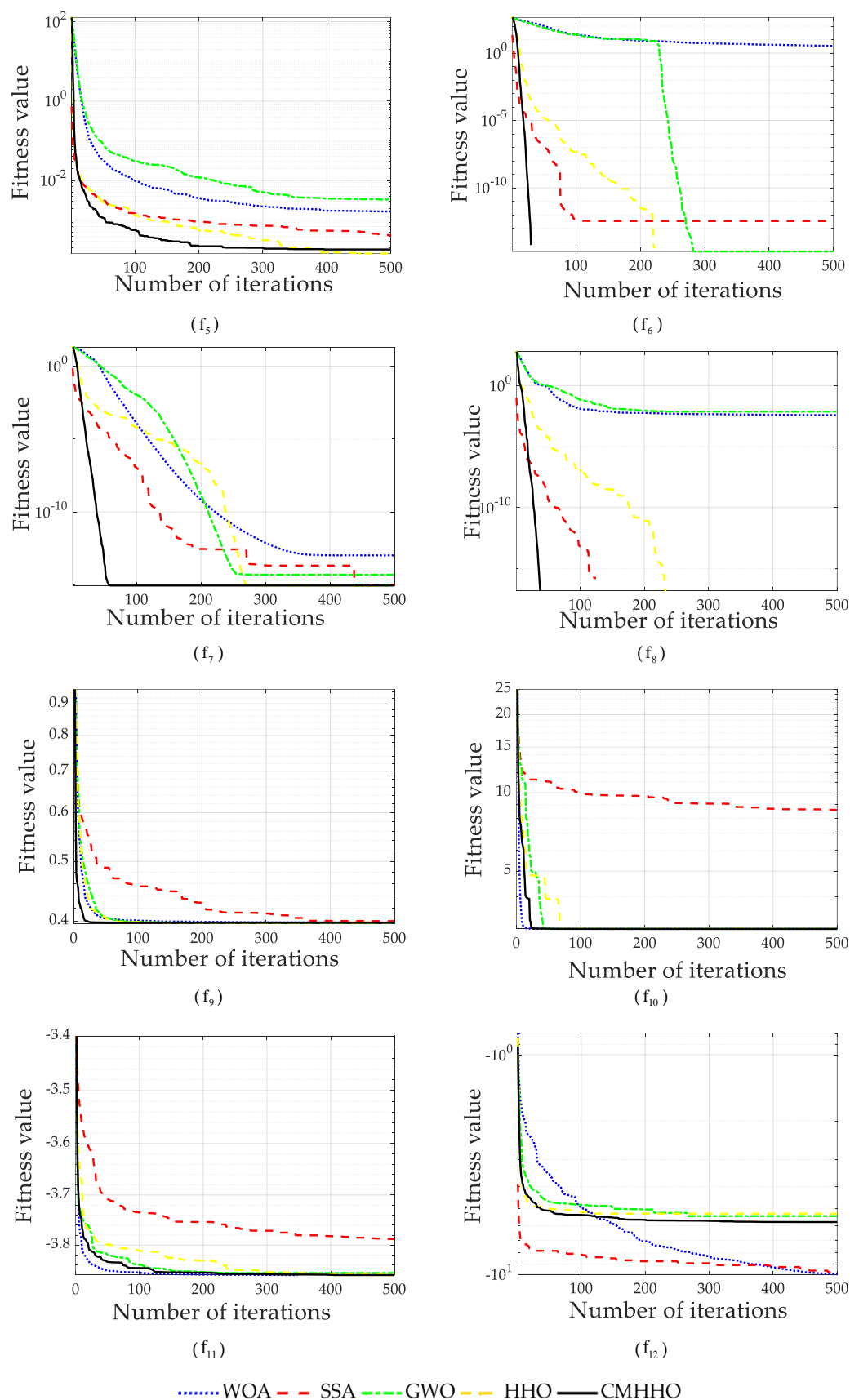
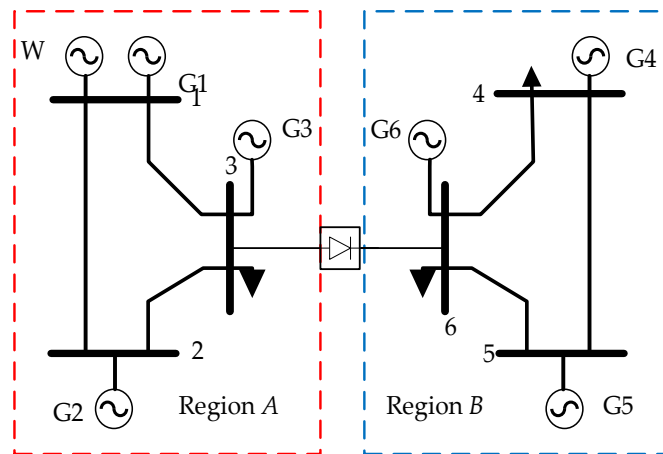


Figure 7. Convergence curves of the five algorithms.

6.2. Simulation Experiment of Two-Region 6-Node Interconnected System

A two-region 6-node interconnected system was considered. The interconnected system included a region A and a region B, connected by a DC tie-line between regions. The DC converter stations were located at node 3 of region A and node 3 of region B. The interconnection system contained a wind farm, located at node 1 of region A. The structure of the two-region 6-node interconnected power system is shown in Figure 8. The line data and thermal power unit data are given in [53]. To ensure that the DC tie-line power flows from region A to region B, the load of region B was 1.2 times that of region A, and the consumption coefficient of the thermal power unit in region B was twice that of the unit in region A. The upper and lower limits of DC transmission were 50 MW and 150 MW. The daily planned exchange of electricity between regions was 1500 MWh. It was assumed that deviation in the DC transmission capacity is not allowed ($\rho = 0$). The output adjustment rate of the DC equivalent generator was in the range of [10,30] MW. The following parameters were set: $\varepsilon = 0.33\%$, $\gamma = 1.5$, $\alpha_{m,t} = \beta_{m,t} = \alpha_{n,t} = \beta_{n,t} = 0.5$ and $\tilde{S}_{m,t}^{dc*} = \tilde{S}_{n,t}^{dc*} = 0$. The load output power forecast values are shown in Figure 9. The wind power forecast values and the upper and lower limits of wind output power values are shown in Figure 10.



Region A and Region B are two areas in two-region 6-node interconnected system

Figure 8. The structure of the two-region 6-node interconnected power system.

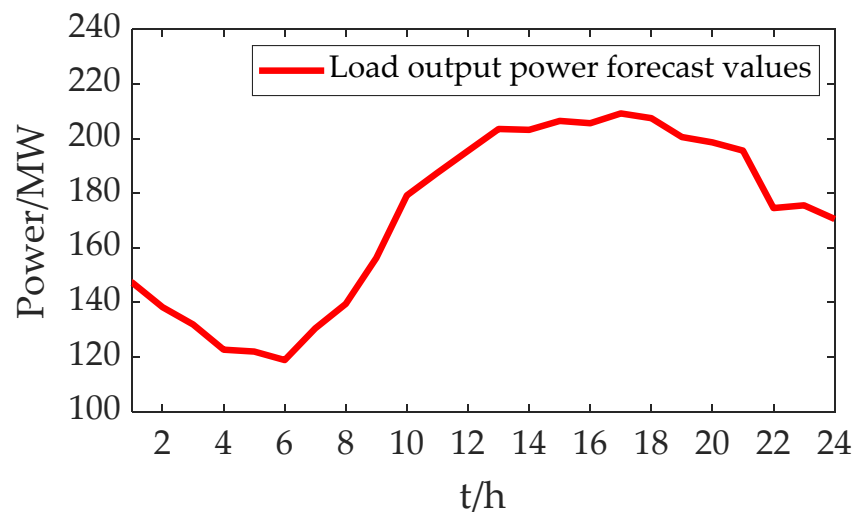


Figure 9. Load output power forecast values.

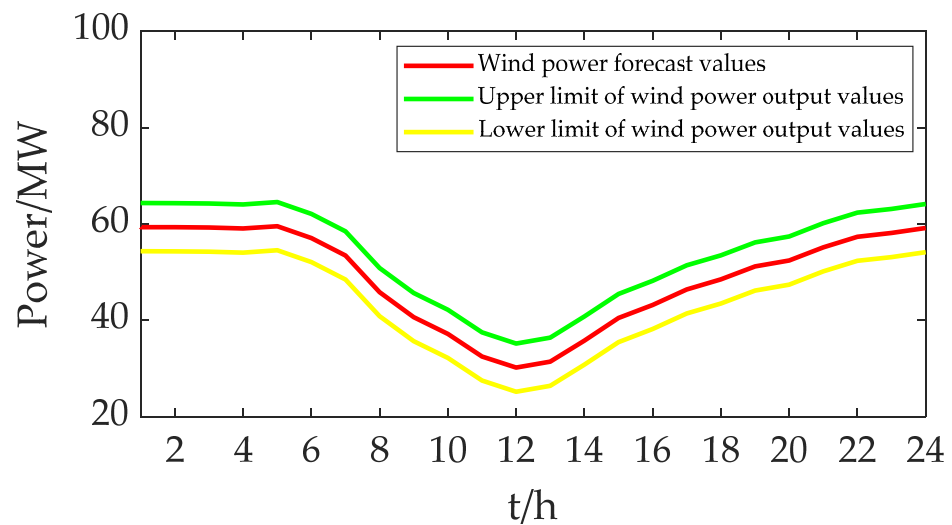


Figure 10. Wind power forecast values and upper and lower limits of wind output power values.

In order to analyze the advantages of flexible adjustment of the DC tie-line power, two DC transmission modes were set and compared.

Mode 1: The DC tie-line operates in the traditional mode, that is, a constant power mode, with less transmission during the load valley period and more transmission during the load peak period.

Mode 2: The flexible operation characteristics of the DC tie-lines are considered, and the DC tie-line power is uniformly optimized.

The DC tie-line transmission plans for the two transmission modes are shown in Figure 11. During the low-load period, the DC tie-line power in Mode 2 is higher than in Mode 1. This shows that Mode 2 is beneficial for transferring the surplus wind power from region A to region B during a trough period. By optimizing the transmission power of the DC tie-line, the cross-regional consumption of wind power resource can be realized, the wind power accommodation capacity of the interconnected power grid is effectively improved and the wind abandonment is reduced.

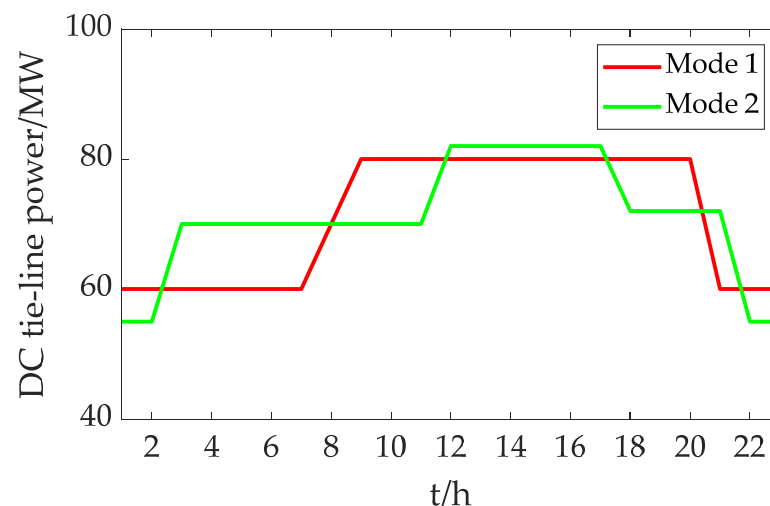


Figure 11. DC tie-line transmission plan in two transmission modes.

The wind abandonment rates and the total power generation costs in the two modes are shown in Table 3. Compared with Mode 1, Mode 2 reduces the wind curtailment of the system and the total power generation cost of the system, indicating that optimizing the

operation mode of the DC tie-line can effectively improve the wind power consumption capacity and the operation economy of the interconnected system.

Table 3. The wind abandonment rates and the total power generation costs in the two modes.

Mode	Total Power Generation Cost/USD	Wind Abandonment Rate/%
Mode 1	86,482.82	7.56
Mode 2	86,120.64	1.32

In order to analyze the superiority of decentralized coordinated dispatch, in the case of Mode 2, two dispatch modes were set up for comparative analysis. The total power generation costs, wind abandonment rates and calculation times of the system for the two dispatch modes are shown in Table 4.

Table 4. Total power generation costs, wind abandonment rates and calculation times of the system in two dispatch modes (two-region 6-node interconnected system).

Mode	Total Power Generation Cost/USD	Wind Abandonment Rate/%	Calculation Times
Centralized dispatch	86,180.64	1.32	13.4
Decentralized dispatch	86,409.75	1.32	52.4

The wind abandonment rate for decentralized dispatch is same as for centralized dispatch, since the tie line exchange power plan is the same for the two dispatch modes. The total power generation cost for decentralized dispatch is slightly higher than for centralized dispatch, but the error is only 0.36%. For small cases such as this, the computation time for decentralized dispatch is higher than for centralized dispatch. This is because decentralized dispatch needs multiple iterations to obtain the global optimal solution, so the solving process is more time-consuming. It should be noted that the purpose of decentralized dispatching is to maintain the independence of each regional grid in an interconnected system. In order to verify the superiority of the CMHHO algorithm for solving this model, the GWO, WOA, SSA, HHO and CMHHO algorithms were all used to solve the case. The total power generation costs and calculation times of the five algorithms are shown in Table 5.

Table 5. Comparison of test results of different algorithms (two-region 6-node interconnected system).

Algorithm	Total Power Generation Cost/USD	Calculation Time/s
WOA	87,834.24	53.2
SSA	87,047.62	51.3
GWO	88,945.48	54.1
HHO	87,652.48	51.7
CMHHO	86,409.75	52.4

It can be seen from Table 5 that the CMHHO algorithm has the best total cost and the strongest optimization ability compared with the WOA, GWO, SSA and traditional HHO algorithms. The calculation time of the CMHHO algorithm is less than that of the GWO algorithm and the WOA algorithm and slightly higher than that of the SSA and traditional HHO algorithm, which is due to the complex iterative process of the CMHHO algorithm. The traditional HHO algorithm and the CMHHO algorithm take a longer time and have a poorer optimization performance than the SSA. However, the CMHHO algorithm has better optimization performance than the HHO algorithm and the SSA. In summary, the CMHHO algorithm is more suitable for solving the proposed model and has a good effect on the decentralized coordinated dispatch problem for interconnected power systems with wind power integration.

6.3. Simulation Experiment for Two-Region 78-Node Interconnected System

To further verify the effectiveness of the decentralized coordination algorithm, a two-area 78-node interconnected system was considered. The interconnected system included two modified New England 39-node systems. These two modified New England 39-node systems modeled region *A* and region *B* and were connected by a DC tie-line between the regions. The interconnected system included 3 wind farms, 20 thermal power units, 78 nodes and 92 lines. A DC converter station was located at node 9 of region *A* and node 9 region *B*. The wind farms were located at nodes 5, 14, and 17 of region *A*. The line data and thermal power unit data are given in [54,55]. The upper and lower limits of DC transmission were 500 MW and 1000 MW. The daily planned exchange of electricity between regions was 20 GWh. It was assumed that deviation in the DC transmission capacity is allowed ($\rho = 2\%$). The output adjustment rate of the DC equivalent generator was in the range of [50, 100] MW. The following parameters were set: $\gamma = 1.2$, $\alpha_{m,t} = \beta_{m,t} = \alpha_{n,t} = \beta_{n,t} = 0.5$ and $\tilde{S}_{m,t}^{dc*} = \tilde{S}_{n,t}^{dc*} = 0$. Different convergence accuracies were set for comparison.

The total generation cost and the calculation time of the system under the two scheduling methods are shown in Table 6. The total power generation cost for decentralized dispatch is basically consistent with centralized dispatch, and when the convergence accuracy of the decentralized coordination algorithm is smaller, the power generation cost is lower. Compared with the results in Table 4 in Section 6.2, the calculation time for decentralized dispatch is basically consistent with that in centralized dispatch. Since a single CPU is used to simulate parallel computing, the advantage of decentralized computing is not obvious. When parallel computing is properly adopted for large-scale power grids, the advantage of decentralized dispatch with regard to computing time is very obvious. From the dispatch results, centralized dispatch and decentralized dispatch are basically the same, but the centralized dispatch has the problems of insufficient communication ability and information privacy, and hence decentralized dispatch is more suitable for China's hierarchical and partitioned power grid dispatch mode.

Table 6. Total power generation costs, convergence accuracy and calculation times of the system in two dispatch modes (two-region 78-node interconnected system).

Mode	Convergence Accuracy	Total Power Generation Cost/USD	Calculation Time
Centralized dispatch	-	2,227,549.8	156.4
Decentralized dispatch	2%	2,230,217.5	164.2
	1%	2,228,953.4	167.8

With $\varepsilon = 2\%$, the total power generation costs and calculation times of the five algorithms are shown in Table 7. It can be seen from Table 7 that compared with the other algorithms, the CMHHO algorithm has the lowest cost and lowest computation time. The CMHHO algorithm is more suitable for solving the decentralized coordinated dispatch problem for interconnected power systems with wind power.

Table 7. Comparison of test results of different algorithms (two-region 78-node interconnected system).

Algorithm	Total Power Generation Cost/USD	Calculation Time/s
WOA	2,354,865.4	167.1
SSA	2,305,465.5	160.8
GWO	2,275,864.9	168.4
HHO	2,315,124.4	162.5
CMHHO	2,230,217.5	164.2

6.4. Experimental Analysis

6.4.1. Superiority of CMHHO Algorithm

Using the five comparison algorithms, the optimization performance of the CMHHO algorithm was compared with those of the other algorithms and analyzed in the MATLAB environment. The main findings of the algorithm comparison experiment were as follows:

- For unimodal functions, the CMHHO algorithm has better convergence accuracy and convergence speed.
- For multimodal functions, the CMHHO algorithm has better convergence speed.
- For multimodal functions with fixed dimensions, the CMHHO algorithm can jump out of local optima.

In summary, the CMHHO algorithm has better convergence precision and convergence speed than the HHO algorithm, and it increases the probability of jumping out of a local optimum. Through the algorithm comparison experiment, the superiority of the CMHHO algorithm was verified.

6.4.2. Effectiveness of the Proposed Model

Regarding the simulation experiments for a two-region 6-node interconnected system and a two-region 78-node interconnected system, the main findings of the simulation analysis were as follows:

- Through the optimization of the DC tie-line, the ability of the interconnected system to absorb wind power is effectively improved, and the wind curtailment is reduced.
- The total power generation cost for decentralized dispatch is basically consistent with that for centralized dispatch, and when the convergence accuracy of the decentralized coordination algorithm is smaller, the power generation cost is lower. It should be noted that the purpose of decentralized dispatching is to maintain the independence of each regional grid in the interconnected system.
- The computation time for decentralized dispatch is higher than that for centralized dispatch. This is because decentralized dispatch needs multiple iterations to obtain the global optimal solution, so the solving process is more time-consuming. Since a single CPU is used to simulate parallel computing, the advantage of decentralized computing is not obvious. When parallel computing is properly adopted for large-scale power grids, the advantage of decentralized dispatch with regard to computing time is very obvious.

In summary, compared with existing research, the model proposed is of great significance for solving the economic dispatch problem for interconnected systems with wind power integration.

6.4.3. Applicability of CMHHO Algorithm to the Proposed Model

Different algorithms were used to solve the two interconnected systems, and the results showed that the CMHHO algorithm has the lowest cost and lowest computation time. This shows that the CMHHO algorithm is more suitable for solving the proposed model.

Through the algorithm comparison experiment and the simulation experiments for the two cases, the superiority of the CMHHO algorithm, the effectiveness of the proposed model and the applicability of the CMHHO algorithm to the proposed model were verified. The proposed model is of great significance for solving the economic dispatch problem for an interconnected system with wind power integration, and is more suitable for the current situation of large-scale, high-concentration and long-distance wind power in China.

7. Conclusions and Future Directions

Aiming at the economic dispatch of interconnected systems with wind power integration, this paper mainly makes the following points:

1. In this paper, the branch cutting method is used to decompose the interconnected region, the DC tie-line is used as the coupling variable and the regional coupling constraints are given.
2. According to the principle of ATC, a decentralized coordination dispatch model based on the CMHHO algorithm is established.
3. In the model proposed in this paper, a virtual upper-level dispatch center is built, and the economic dispatch problem is divided into a master optimization problem for the upper-level dispatch center and subsidiary optimization problems for the lower-level dispatch centers. The upper-level dispatch center is responsible for coordinating the DC tie-line power flow to the interconnected regions, and the lower-level dispatch centers solve their own economic dispatch problems in a parallel manner.
4. The optimization objective, mathematical formula and constraints of the model are given.
5. For solving the model, the HHO algorithm is introduced, and a CMHHO algorithm that improves the HHO algorithm in three respects is proposed. The improvements are as follows:
 - (1) A new nonlinear escape energy factor renewal strategy is proposed to balance the exploitation and exploration of the algorithm.
 - (2) A chaotic tent map is used to adjust the key parameters of the algorithm to enhance the diversity of the population.
 - (3) The "DC/Pbad-to-Pbest/1" strategy is used to impose a global mutation operation on the population, to avoid the algorithm falling into a local optimum. In order to verify the superiority of the CMHHO algorithm, the effectiveness of the proposed model and the applicability of the CMHHO algorithm to the proposed model, an algorithm comparison experiment and the simulation analysis of two interconnected system cases are completed.

Aiming at the economic dispatch problem of interconnected systems with wind power integration, in this paper, a decentralized coordination dispatch model based on the CMHHO algorithm was established. Through an algorithm comparison experiment and simulation of two interconnected system cases, the superiority of the CMHHO algorithm, the effectiveness of the proposed model and the applicability of the CMHHO algorithm to the proposed model were verified. The model proposed is of great significance for solving the economic dispatch problem for interconnected systems with wind power integration, and is more suitable for the current situation of large-scale, high-concentration and long-distance wind power in China.

The future research directions will be mainly to consider factors such as wind power uncertainty in the decentralized coordinated dispatch of multi-regional power systems with wind power integration and to reduce the CMHHO algorithm operating time.

Author Contributions: Conceptualization, Y.W.; methodology, Y.W.; software, Y.W.; validation, Y.W.; formal analysis, Y.W.; writing—original draft preparation, Y.W.; writing—review and editing, Z.Y., Z.D. and R.X.; supervision, M.Q., Y.Z. and L.L. All authors have read and agreed to the published version of the manuscript.

Funding: This research was funded by the Youth project of Shandong Natural Science Foundation of China, Funding number: (ZR2017LEE022). Funder: Z.D. and The Key Research and Development Program of Zibo, Shandong, China, Funding number (2019ZBXC498). Funder: Z.D.

Institutional Review Board Statement: Not applicable.

Informed Consent Statement: Not applicable.

Data Availability Statement: Not applicable.

Conflicts of Interest: The authors declare no conflict of interest.

References

1. Wei, Y.; Wang, J.; Li, N. An Analysis of the Influence of Grid-Connected Renewable Energy on Power Quality of Power Grids. *Power Syst. Clean Energy* **2022**, *38*, 108–114.
2. Wang, Y.; Zhu, S.; Chen, F.; Zhou, S. A Preliminary Study on the Coordinated Development of Nuclear and Renewable Energy Power Generation in China. *Renew. Energy Resour.* **2021**, *39*, 1069–1077.
3. Huang, T.; Shang, B. Assessment and Supervision of Renewable Portfolio Standards and Strategic Selection of Stakeholders. *Resour. Sci.* **2020**, *42*, 2393–2405. [[CrossRef](#)]
4. Wang, C.; Wang, S. Study on Some Key Problems Related to Distributed Generation System. *Autom. Electr. Power Syst.* **2018**, *32*, 1–4+31.
5. Hu, Q.; Cao, Y. Dynamic Low-carbon Dispatching Model Based on Improving PSO and GA. *J. Shanghai Univ. Electr. Power* **2022**, *38*, 9–16.
6. Xie, Y.; Teng, X.; Zheng, T.; Chen, L. Analysis of Economic Influence Factors in Wind-Photovoltaic-Storage Microgrid. *Autom. Electr. Power Syst.* **2019**, *43*, 70–76, 115.
7. Xia, P.; Liu, W.; Zhang, Y.; Wang, W.; Zhang, B. A Distributionally Robust Optimization Scheduling Model Considering Higher-order Uncertainty of Wind Power. *Trans. China Electrotech. Soc.* **2020**, *35*, 189–200.
8. Shao, X. Influence of Wind Power Grid Connection on Power System Dispatching Operation. *Electron. Compon. Inf. Technol.* **2020**, *4*, 94–95.
9. He, P.; Chi, F.; Zhao, Z.; Liu, C.; Li, G.; Wang, Z. Research on Two-stage Scheduling of Wind Energy Storage System with Demand Response Participation. *Comput. Digit. Eng.* **2019**, *49*, 1936–1944.
10. Jing, J.; Li, C.; Peng, C.; Feng, J.; Zhao, Y. Low-carbon Power Dispatch with Wind Power. *J. Nanning Univ. Aeronaut. Astronaut. Soc. Sci.* **2017**, *19*, 10–17.
11. Yu, D.; Yang, M.; Han, X.; Ma, S.; Liu, D. Robust Real-time Dispatch Considering Probabilistic Distribution of Wind Generation. *Proc. CSEE* **2017**, *37*, 727–738.
12. Shi, Y.; Guo, C. Flexibility Reinforcement Method for Integrated Electricity and Heat System Based on Decentralized and Coordinated Multi-stage Robust Dispatching. *Autom. Electr. Syst.* **2022**, *46*, 10–19.
13. Li, P.; Chen, B.; Wang, Z.; Zhou, F.; Wu, D.; Liu, Y. Decentralized coordinated dispatch of multi-community integrated energy system considering network security constraints and multi-energy collaborative interaction. *Electr. Power Autom. Equip.* **2022**, *40*, 15–25.
14. Guo, Z.; Li, G.; Zhou, M.; Wang, J. A Decentralized and Robust Optimal Scheduling Model of Integrated Electricity-gas System for Wind Power Accommodation. *Proc. CSEE* **2020**, *40*, 6442–6455.
15. Chen, L. Research on Load Balancing and Decentralized Dispatching Method of Renewable Energy Power System. *Power Syst. Clean Energy* **2019**, *35*, 60–66.
16. Su, L.; Li, Z.; Zhang, Z.; Du, Y.; Ge, X.; Yang, X. A coordinated operation strategy for integrated energy microgrid clusters based on chance-constrained programming. *Power Syst. Prot. Control.* **2021**, *49*, 123–131.
17. Ding, X.; Guo, C. Decentralized Synergetic Dispatching Method for Multi-microgrid under Market Environment. *Mod. Electr. Power* **2020**, *37*, 221–230.
18. Cheng, S.; Shang, D.; Zhong, S. Hybrid Decentralized Optimization of Dispatching Electrical Units with Consideration of Demand-side Response. *Adv. Eng. Sci.* **2021**, *53*, 235–242.
19. Yan, J.; Zhou, L.; Zheng, H.; Chen, C.; Jiang, C. Chance-constrained Distributed Control of Distribution Network Power Sources Based on Augmented Lagrangian Alternating Direction Inexact Newton Method. *Sci. Technol. Eng.* **2022**, *22*, 3160–3168.
20. Ma, F.; Zhang, B.; Gong, C.; Jiao, R.; Wang, J. Decentralized stochastic dispatch approach for multi-area power system considering wind power uncertainty. *Electr. Meas. Instrum.* **2019**, *56*, 68–74.
21. Wu, Z. Research on the Superiority of Swarm Intelligence Algorithm in the Era of Big Data. *Wirel. Internet Technol.* **2019**, *16*, 110–111.
22. Lin, S.; Dong, C.; Chen, M.; Zhang, F.; Chen, J. Summary of new group intelligent optimization algorithms. *Comput. Eng. Appl.* **2018**, *54*, 13–15.
23. Liu, X.; Tian, Y.; Tian, Y. A Survey of Swarm Intelligence Methods. *China Comput. Commun.* **2021**, *33*, 63–69.
24. Kumar, N.K.; Gopi, R.S.; Kuppusamy, R.; Nikolovski, S.; Teekaraman, Y.; Vairavasundaram, I.; Venkateswarulu, S. Fuzzy Logic-Based Load Frequency Control in an Island Hybrid Power System Model Using Artificial Bee Colony Optimization. *Energies* **2022**, *15*, 2199. [[CrossRef](#)]
25. Al-Tameemi, Z.H.A.; Lie, T.T.; Foo, G.; Blaabjerg, F. Optimal Coordinated Control Strategy of Clustered DC Microgrids under Load-Generation Uncertainties Based on GWO. *Electronics* **2022**, *11*, 1244. [[CrossRef](#)]
26. Bai, J.; Tian, M.; Li, J. Control System of Liquid Fertilizer Variable-Rate Fertilization Based on Beetle Antennae Search Algorithm. *Processes* **2022**, *10*, 357. [[CrossRef](#)]
27. Hameed, K.; Khan, W.; Abdalla, Y.S.; Al-Harbi, F.F.; Armghan, A.; Asif, M.; Salman Qamar, M.; Ali, F.; Miah, M.S.; Alibakhshikani, M.; et al. Far-Field DOA Estimation of Uncorrelated RADAR Signals through Coprime Arrays in Low SNR Regime by Implementing Cuckoo Search Algorithm. *Electronics* **2022**, *11*, 558. [[CrossRef](#)]
28. Lu, X.; Li, C.; Wu, Z. Microgrid Fault Diagnosis Based on Extreme Learning Machine Optimized by Whale Algorithm. *Smart Power* **2022**, *50*, 15–21.

29. Lee, Y.-D.; Lin, W.-C.; Jiang, J.-L.; Cai, J.-H.; Huang, W.-T.; Yao, K.-C. Optimal Individual Phase Voltage Regulation Strategies in Active Distribution Networks with High PV Penetration Using the Sparrow Search Algorithm. *Energies* **2021**, *14*, 8370. [[CrossRef](#)]
30. Qing, X.; Luo, G.; Li, W.; Zhang, G. A Review of Swarm Intelligence Algorithms. *Unmanned Syst. Technol.* **2021**, *4*, 1–10.
31. Jia, H.; Kang, L.; Sun, K.; Peng, X.; Li, Y.; Jiang, Z. Harris hawk algorithm for optimizing pulse coupled neural network for automatic image segmentation. *Appl. Sci. Technol.* **2019**, *46*, 16–20+25.
32. Wang, G.; Tian, Z. Short-term Hydrothermal Scheduling Based on Mutation and Hierarchy-based Hybridization Strategy. *Electr. Eng. Mater.* **2021**, *3*, 58–62.
33. Wu, D.; Wen, L. An Improved BP Neural Network Based on Harris Hawks Algorithm. *Netw. Secur. Technol. Appl.* **2022**, *1*, 38–40.
34. Kashif, H.; William, Z.; Najib, M.S. Long-Term Memory Harris' Hawk Optimization for High Dimensional and Optimal Power Flow Problems. *IEEE Access* **2019**, *7*, 147596–147616.
35. Elgamel, Z.M.; Binti, N.; Tubishat, M.; Alswaitti, M.; Mirjalili, S. An Improved Harris Hawks Optimization Algorithm with Simulated Annealing for Feature Selection in the Medical Field. *IEEE Access* **2020**, *8*, 186638–186652. [[CrossRef](#)]
36. Ma, Y.; Shi, Z.; Zhao, K.; Gong, C.; Shan, L. TDOA location based on improved Harris Eagle optimization algorithm. *Comput. Eng.* **2020**, *46*, 179–184.
37. Qu, C.; He, W.; Peng, X.; Peng, X. Harris Hawks Optimization with Information Exchange. *Appl. Math. Model.* **2020**, *84*, 52–75. [[CrossRef](#)]
38. Guo, Y.; Liu, S.; Gao, W.; Zhang, L. Elite Opposition-Based Learning Golden-Sine Harris Hawks Optimization. *Comput. Eng. Appl.* **2021**, *accepted*.
39. Xia, Y.; Zhu, J. Decentralized Optimal Dispatch of Multi-Area Power Systems Based on Analytical Target Cascading. *Electrotech. Electr.* **2020**, *11*, 10–15.
40. Liu, D.; Zhu, J.; Zhao, W.; Liu, Y.; Li, N.; Gao, S.; Li, A. Multi Source Optimal Dispatching of Super-high Power Regenerative Electro Boilers with Thermal Power Unit Depth Regulation. *Jilin Electr. Power* **2022**, *50*, 24–28.
41. Liu, D.; Ma, C.; Wang, Y. Joint Optimal Control of Maximum Wind Power Consumption. *Distrib. Energy* **2021**, *6*, 21–26.
42. Li, J.; Xie, M.; Li, S.; Lin, S.; Huang, B. Optimal Dispatch of Unit Commitment and Multi-Scenario Reserve Decision Considering CVaR. *South. Energy Constr.* **2021**, *8*, 50–65.
43. Yuan, G.; Jia, X.; Fang, F.; Dong, J. Joint Stochastic Optimal Scheduling of Heat and Power Considering Source and Load Sides of Virtual Power Plant. *Power Syst. Technol.* **2020**, *44*, 2932–2940.
44. Xu, H.; Li, H. Planning and Operation Stochastic Optimization Model of Power Systems Considering the Flexibility Reformation. *Power Syst. Technol.* **2020**, *44*, 4326–4638.
45. Ma, S.; Ren, Y.; Fan, Y.; Meng, F. DC Communication Line Power Optimization Method Considering Reactive Power Regulation Cost. *Electr. Eng.* **2021**, *11*, 71–74+79.
46. Wang, L.; Zhang, J. Optimal scheduling method for an inter-regional DC grid system based on fuzzy chance constrained programming. *Power Syst. Prot. Control.* **2021**, *49*, 12–19.
47. Xiao, J.; Zhang, K.; Gao, F.; Zhang, Z.; Gu, W. Pitch diameter measurement of threaded steel wire head based on HHO algorithm. *J. Electron. Meas. Instrum.* **2021**, *10*, 48–55.
48. Xu, G.; Liu, M. Malware Detection Method Based on Improved Harris Hawks Optimization Synchronization Optimization Feature Selection. *Netinfo Secur.* **2021**, *21*, 9–18.
49. Zhang, J.; Wang, X.; Lu, L.; Niu, P. Analysis and Research of Several New Intelligent Optimization Algorithms. *J. Front. Comput. Sci. Technol.* **2022**, *16*, 88–105.
50. Li, Y.; Han, M.; Guo, Q. Modified Whale Optimization Algorithm Based on Tent Chaotic Mapping and Its Application in Structural Optimization. *KSCE J. Civ. Eng.* **2020**, *24*, 1–11. [[CrossRef](#)]
51. Tong, L. *Research on Differential Evolution-Based Intelligent Optimization Algorithms*; Guilin University of Technology: Guilin, China, 2018.
52. Kargarian, A.; Fu, Y.; Li, Z. Distributed Security-constrained Unit Commitment for Large-scale Power Systems. *IEEE Trans. Power Syst.* **2015**, *30*, 1925–1936. [[CrossRef](#)]
53. Zhu, T.; Zhu, J.; Liu, M.; Zhao, W. Decentralized Stochastic Optimization Method for Dynamic Economic Dispatch of Power System with Wind Farms. *Autom. Electr. Power Syst.* **2017**, *41*, 48–54.
54. Nguyen, T.; Pai, M.A. Dynamic security-constrained rescheduling of power systems using trajectory sensitivities. *IEEE Trans Power Syst.* **2003**, *18*, 848–854. [[CrossRef](#)]
55. Zimmerman, R.D.; Murillo-Sánchez, C.E.; Thomas, R.J. MATPOWER: Steady-state operations, planning, and analysis tools for power systems research and education. *IEEE Trans Power Syst.* **2011**, *26*, 12–19. [[CrossRef](#)]